Published in final edited form as:
Traffic. 2011 July ; 12(7): 912–924. doi:10.1111/j.1600-0854.2011.01203.x.

Disruption of the Man-6-P Targeting Pathway in Mice Impairs Osteoclast Secretory Lysosome Biogenesis

Eline van Meel[#,*], **Marielle Boonen**[#,‡], **Haibo Zhao**[+,§], **Viola Oorschot**[*], **F. Patrick Ross**[+], **Stuart Kornfeld**[‡], and **Judith Klumperman**[*]

[*] Department of Cell Biology, University Medical Center Utrecht, Heidelberglaan 100, 3584 CX Utrecht, the Netherlands [‡] Department of Internal Medicine, Washington University School of Medicine, St. Louis, MO 63110, USA [+] Department of Pathology and Immunology, Washington University School of Medicine, St. Louis, MO 63110, USA

Abstract

Osteoclasts are specialized cells that secrete lysosomal acid hydrolases at the site of bone resorption, a process critical for skeletal formation and remodeling. However, the cellular mechanism underlying this secretion and the organization of the endo-lysosomal system of osteoclasts have remained unclear. We report that osteoclasts differentiated *in vitro* from murine bone-marrow macrophages contain two types of lysosomes. The major species is a secretory lysosome containing cathepsin K and tartrate-resistant acid phosphatase (TRAP), two hydrolases critical for bone resorption. These secretory lysosomes are shown to fuse with the plasma membrane, allowing the regulated release of acid hydrolases at the site of bone resorption. The other type of lysosome contains cathepsin D, but little cathepsin K or TRAP. Osteoclasts from *Gnptab*$^{-/-}$ mice, which lack a functional mannose 6-phosphate targeting pathway, show increased secretion of cathepsin K and TRAP and impaired secretory lysosome formation. However, cathepsin D targeting was intact, showing that osteoclasts have a mannose 6-phosphate-independent pathway for selected acid hydrolases.

Keywords

Osteoclasts; Mannose 6-Phosphate; Secretory lysosomes; Cathepsin K; CathepsinD

INTRODUCTION

Osteoclasts are multinucleated cells specialized in bone resorption that differentiate from hematopoietic mononuclear precursor cells (reviewed by 1–3). When osteoclasts contact bone, they polarize to form a convoluted membrane, the ruffled border. The ruffled border forms within an actin ring, generating an isolated, acidic extracellular microenvironment (the resorption lacuna), into which acid hydrolases are secreted. Two acid hydrolases that are highly expressed and secreted by differentiated osteoclasts are cathepsin K and tartrate-resistant acid phosphatase (TRAP, also known as ACP5, or uteroferrin). Cathepsin K is a cysteine protease that degrades type I collagen, the major component of bone matrix (4, 5).

Correspondence to Judith Klumperman: Department of Cell Biology, University Medical Center Utrecht, Heidelberglaan 100, 3584 CX Utrecht, the Netherlands, phone +31-88-7556550, fax +31-30-2541797, j.klumperman@umcutrecht.nl.
[§]Current address: Center for Osteoporosis and Metabolic Bone Diseases, University of Arkansas for Medical Sciences, Little Rock, AR 72205, USA
[#]Authors contributed equally

TRAP is a metallophosphoesterase involved in bone matrix degradation (6, 7) and removal of mannose 6-phosphate (Man-6-P) residues from acid hydrolases (8).

Acid hydrolase secretion by osteoclasts is a key regulatory mechanism for skeletal formation and remodeling. Nonetheless, the cellular mechanism that underlies this secretion has remained unclear. Two models have been proposed. In one model, newly synthesized acid hydrolases at the TGN are packaged into transport vesicles that deliver their cargo directly to the ruffled border (9–11). The alternative model proposes that acid hydrolases are first transported from the TGN to endo-lysosomes that subsequently fuse with the ruffled border to discharge their contents (12–16). However, the characterization of the endo-lysosomal compartments in osteoclasts is incomplete and their fusion with the plasma membrane has not been directly demonstrated. Furthermore, the requirement of the Man-6-P recognition system for the proper trafficking of cathepsin K, TRAP and other acid hydrolases by Man-6-P receptors (MPRs) has not been investigated in osteoclasts.

In this study we utilize immuno-EM and biochemical assays to determine the subcellular localization and transport pathways of cathepsin K, TRAP and the ubiquitously expressed acid hydrolase cathepsin D. Osteoclasts were derived from both wild type (WT) and *Gnptab*$^{-/-}$ mice, which lack the catalytic α,β-subunits of GlcNAc-1-phosphotransferase (17) and are unable to add Man-6-P residues to newly synthesized lysosomal hydrolases (18). Our data show that osteoclasts contain secretory lysosomes, which are compartments with all the characteristics of lysosomes, but that undergo regulated secretion in response to external stimuli (19). These secretory lysosomes are responsible for the activation and transport of cathepsin K and TRAP to the ruffled border. Interestingly, our study reveals that, in addition to secretory lysosomes, osteoclasts contain a second type of lysosome that is enriched in cathepsin D, but contains very little cathepsin K and TRAP. Finally, we demonstrate that the targeting of cathepsin K and TRAP to secretory lysosomes is Man-6-P-dependent, while the lysosomal targeting of cathepsin D does not require this pathway.

RESULTS

Cathepsin K and TRAP co-localize in secretory lysosomes that fuse with the plasma membrane

To study the intracellular targeting of cathepsin K and TRAP in osteoclasts, mouse bone-marrow derived macrophages were differentiated *in vitro* into mature osteoclasts on a plastic substrate. First we determined the subcellular localization of cathepsin K by immuno-EM on ultrathin cryosections of WT osteoclasts. This protease was found in endosomes (defined by their electron lucent lumen and presence of intraluminal vesicles) (Figure 1A) and most prominently in electron-dense, lysosome-like compartments of 200–900 nanometer (nm) diameter (Figure 1A). In the biosynthetic pathway cathepsin K was found in the ER, Golgi and TGN (Figure 1A and 3A).

To better characterize the cathepsin K-enriched lysosome-like compartments, osteoclasts were incubated with BSA conjugated to 5 nm gold particles. Endocytosed BSA-gold was detected in these compartments after 3 h (Figure 1B) but not after 30 min of uptake. These kinetics position them in the late stage of the endosomal pathway (20). To further confirm the lysosomal nature of these compartments, we performed double-immunogold labeling for cathepsin K and the lysosomal membrane protein LAMP-2. This resulted in labeling of the limiting membrane of the cathepsin K-positive compartments (Figure 1C–D), consistent with them being lysosomes. Interestingly, we regularly observed patches of cathepsin K labeling at the exterior of the plasma membrane with a diameter similar to the intracellular cathepsin K-enriched compartments (Figure 1B and 1E–F). These patches also contained BSA-gold, whereas the underlying plasma membrane regions labeled for LAMP-2 (Figure

1E), identifying them as fusion profiles of the cathepsin K/BSA-gold positive compartments. Together, these characteristics of the dense, cathepsin K-containing compartments meet the definition of 'secretory lysosome' (19, 21, 22). Immuno-EM of TRAP resulted in fewer gold particles, but a similar localization pattern as for cathepsin K with a clear enrichment in secretory lysosomes, where it co-localized with cathepsin K (Figure 2A–C). Thus, our combined EM data show that TRAP and cathepsin K accumulate and co-localize in secretory lysosomes.

If secretory lysosomes mediate secretion of acid hydrolases it is predicted that the secreted enzymes will be largely devoid of their Man-6-P moiety, since this would have been removed, most likely by TRAP (8), in the acidic milieu of the secretory lysosome. Indeed we found that of several glycosidases secreted by WT osteoclasts only a minor fraction bound to a CI-MPR-affinity column (Supplemental Table I). This binding behavior was similar to that of the intracellular glycosidases, which reside mainly in lysosomes. In further support of this model, we confirmed by immuno-EM the absence of Man-6-P on acid hydrolases in osteoclast secretory lysosomes (Figure S1). These data are all consistent with the model that in osteoclasts acid hydrolases are targeted to secretory lysosomes, where they are processed prior to fusion of the secretory lysosomes with the plasma membrane.

The sorting of cathepsin K and TRAP to secretory lysosomes is Man-6-P-dependent

Both cathepsin K and TRAP acquire Man-6-P modifications in osteoclasts (11). We therefore investigated whether targeting of cathepsin K and TRAP to secretory lysosomes is Man-6-P-dependent. By immuno-EM, cathepsin K label was particularly prominent in electron-dense regions of the Golgi cisternae, indicating high local protein concentrations (Figure 3A, arrowheads). In the TGN, cathepsin K was found in small-sized, electron-dense vesicles (Figure 3A–B, arrows). Similar vesicles were found throughout the cytoplasm and in close proximity to endosomes. The great majority (82 ± 0.3%) of these vesicles were not accessible to BSA-gold (3 h uptake), indicating that they are of biosynthetic origin (Figure 3B). To test whether these vesicles also contain CI-MPR, we performed a double-labeling for cathepsin K and CI-MPR. The CI-MPR was found in the TGN, endosomes and small vesicles dispersed through the cytoplasm, some in close proximity to endosomes (Figure 3C–D), in agreement with its distribution in other cell types (23, 24). Extremely low levels of the CI-MPR were detected in the secretory lysosomes (Figure S2). Cathepsin K and CI-MPR co-localized in endosomes and in a portion of the small vesicles, including those in the TGN and near endosomes (Figure 3C–D). These data are consistent with Man-6-P-dependent targeting of newly synthesized cathepsin K to the endo-lysosomal system.

To further study the Man-6-P dependence of cathepsin K and TRAP targeting to secretory lysosomes we differentiated osteoclasts from macrophages isolated from *Gnptab*$^{-/-}$ mice (17), which fail to generate Man-6-P-residues on newly synthesized lysosomal hydrolases (18). By immuno-EM of these cells, only low levels of cathepsin K were found in endo-lysosomes (Figure 1G), while this protease could be readily detected in the ER, Golgi and TGN (Figure 1H–I). TRAP labeling was also greatly reduced in endo-lysosomes of *Gnptab*$^{-/-}$ osteoclasts (Figure 2D). The number of electron-dense secretory lysosomes was markedly reduced (~2 per cell profile versus ~9 in WT) and the remaining profiles were of smaller size than in WT cells (200–500 nm versus 200–900 nm, respectively). By contrast, there was a marked increase in more electron-lucent compartments containing relatively low levels of cathepsin K (~19 per cell profile versus ~6 in WT cells). By size and morphology these compartments likely represent endosomes and secretory lysosomes that had failed to acquire their full content of cathepsin K (Figure 1G). Concomitantly, they could be reached by BSA-gold after 3 h of uptake (Figure 1I).

Strikingly, much of the cathepsin K in *Gnptab*$^{-/-}$ osteoclasts was found in numerous small, ≤ 200 nm vesicular membrane profiles located in the TGN area and dispersed throughout the cytoplasm (Figure 1H–I). Most of these profiles were not labeled for the ER marker calreticulin and were inaccessible to internalized BSA-gold (3 h uptake), indicating that they are not of ER or endocytic origin (Figure 1H–I). Interestingly, the patches of secreted cathepsin K at the plasma membrane (Figure 1H) were markedly smaller in size than in WT osteoclasts (Figure 1B and 1E–F) with a maximum diameter of ~200 nm, the size of the small, intracellular vesicles. These data suggest that the numerous cathepsin K vesicles present in *Gnptab*$^{-/-}$ osteoclasts represent biosynthetic vesicles that direct cathepsin K directly from the TGN to the plasma membrane via the constitutive secretory pathway.

We then investigated whether the impairment of secretory lysosome biogenesis in *Gnptab*$^{-/-}$ osteoclasts impacted the formation of the resorption lacuna and the targeting of acid hydrolases to this compartment. We cultured WT and *Gnptab*$^{-/-}$ osteoclasts on bone slices to allow formation of the ruffled border and analyzed the presence of cathepsin K within the actin ring by immunofluorescence. Both WT and *Gnptab*$^{-/-}$ cells formed actin rings and exhibited a concentration of cathepsin K inside the resorption lacuna (Figure 4). Together these results suggest that in *Gnptab*$^{-/-}$ osteoclasts at least a portion of the constitutive vesicles that package cathepsin K reach the resorption lacuna.

Disruption of the Man-6-P targeting pathway results in increased secretion of cathepsin K and TRAP by osteoclasts

To further study the lysosomal targeting of cathepsin K, we next determined its steady state level in cell lysates and culture media from WT and *Gnptab*$^{-/-}$ osteoclasts. Western blots of WT cell lysates revealed a doublet at ~25 kD, corresponding to the mature form of cathepsin K (Figure 5A), whereas the proform (~40 kD) was barely detectable. Processing of cathepsin K requires acidic conditions (5). Hence, the presence of mature enzyme indicates its targeting to lysosomes. WT culture medium collected after a 6 h incubation, contained small amounts of mature cathepsin K, but no detectable proform. Since osteoclasts grown on plastic do not form an acidic resorption lacuna, the presence of mature cathepsin K in the medium reflects its targeting to secretory lysosomes followed by processing and release. In *Gnptab*$^{-/-}$ osteoclasts, the steady state intracellular level of mature cathepsin K was markedly reduced, while the proform was now clearly detectable in the medium (Figure 5A). These data, in agreement with our morphological observations, indicate that in the absence of the Man-6-P modification, newly synthesized procathepsin K is secreted via the constitutive secretory pathway, rather than targeted to secretory lysosomes.

We next analyzed the intracellular targeting of TRAP by metabolic pulse/chase studies. TRAP is synthesized as an inactive monomeric ~35 kD proform and processed in the lysosome into a mature enzyme composed of two disulfide-linked subunits (25). WT and *Gnptab*$^{-/-}$ osteoclasts were incubated with ^{35}S-methionine/cysteine for 30 min followed by a 2 h chase in unlabeled medium and subsequent immunoprecipitation of TRAP. In WT cell lysates, the 30 min pulse resulted in the appearance of the ~35 kD proform (Figure 5B, upper panel). After the 2 h chase period, a portion of this proform had been converted into a ~23 kD form, which corresponds to the N-terminal fragment of the 2-subunit mature enzyme (25) (Figure 5B lower panel). The presence of the mature form of TRAP within the cell lysate reflects its targeting to secretory lysosomes. However, the media from the 2 h chase period contained mostly proform of TRAP with only a small amount of the mature form. This observation indicates that in addition to secretion via secretory lysosomes there is considerable secretion of TRAP directly from the TGN. Of note, these autoradiograms underestimate the amount of mature enzyme, because the TRAP proform contains ~3x more methionine/cysteine residues than the 23 kD N-terminal fragment. To obtain an accurate measure of the amount of secreted TRAP, we repeated this experiment using non-reducing

conditions. Quantification of 3 independent experiments revealed that 49 ± 6% of newly synthesized TRAP is secreted within 2 h.

The presence of the mature enzyme in WT cell lysate was confirmed when the steady state level of TRAP was determined by western blotting (Figure 5C). The medium, collected over 6 h, contained low levels of the mature enzyme and only trace amounts of the proform (Figure 5C). Notably, while the proform in the media represents newly synthesized TRAP secreted during the 6 h collection period, most of the mature form likely originates from secretory lysosomes, which have accumulated TRAP over a longer time period. Consequently, the ratio of pro- to mature forms obtained by western blotting differs from the pulse/chase experiment (Figure 5B), which exclusively visualizes newly synthesized TRAP. We conclude from these data that in WT osteoclasts TRAP can be secreted directly from the TGN, as well as via secretory lysosomes.

Pulse/chase experiments with *Gnptab*$^{-/-}$ osteoclasts showed that 68 ± 5.5% of newly synthesized TRAP was secreted within 2 h (compared to 49 ± 6% by the WT cells, n=3, $p<0.01$) (Figure 5B, upper panel). In contrast to the WT cells, the secreted TRAP consisted solely of the proform (Figure 5B, lower panel). Western blotting showed that the intracellular level of mature TRAP was greatly reduced in the *Gnptab*$^{-/-}$ cells (Figure 5C), whereas the medium contained much more proform compared to WT (Figure 5C). These data demonstrate that disruption of the Man-6-P targeting pathway inhibits sorting of both TRAP and cathepsin K to secretory lysosomes, resulting in their increased secretion via the constitutive pathway.

Gnptab$^{-/-}$ osteoclasts also exhibited reduced levels of several lysosomal glycosidases (Supplemental Table II). Since no significant changes of mRNA levels were detected by microarray and RT-PCR analysis (data not shown) this is consistent with their increased secretion.

Gnptab$^{-/-}$ osteoclasts exhibit a Man-6-P-independent transport pathway for cathepsin D

To extend our studies on lysosomal sorting in osteoclasts, we next investigated the lysosomal targeting of another acid hydrolase, cathepsin D. Cathepsin D is a ubiquitously expressed aspartic protease that, in contrast to cathepsin K and TRAP, has not been directly implicated in bone resorption (26). Mouse cathepsin D is synthesized as an inactive ~42 kD proform, which is converted in acidic compartments to the mature ~39 kD protein. Unexpectedly, by western blot analysis, we found that the steady state levels of intracellular and secreted mature cathepsin D were similar in WT and *Gnptab*$^{-/-}$ cells (Figure 5E), suggesting that lysosomal targeting of cathepsin D in osteoclasts is independent of the Man-6-P modification. In agreement herewith, metabolic labeling with ^{35}S-methionine/cysteine (30 min pulse, 4 h chase) resulted in comparable levels of mature cathepsin D in both cell types (Figure 5F). The mature form was also found in the media, where no secreted proform could be detected. The percentage of secreted cathepsin D was similar in both cell types (33 ± 7.9% in WT vs 36 ± 2.6% in *Gnptab*$^{-/-}$, n=6, $p=0.40$). These data indicate that, in contrast to cathepsin K and TRAP, in the absence of the Man-6-P modification cathepsin D is normally targeted to osteoclast lysosomes.

Cathepsin D and cathepsin K localize to different lysosomes in osteoclasts

We further studied the subcellular distribution of cathepsin D by double-labeling cathepsin D and K for immuno-EM. In WT osteoclasts there was low but consistent labeling of cathepsin D in cathepsin K-positive secretory lysosomes (Figure 6A) and their fusion profiles at the plasma membrane (inset Figure 6A). However, additional cathepsin D labeling was found in compartments that contained no or only low levels of cathepsin K

(Figure 6A, arrow). By size and electron density these compartments resembled lysosomes, which was confirmed by the observation that they could be reached by endocytosed BSA-gold after 3 h, but not 30 min, of incubation (Figure 6B). These data show that cathepsin D is present in secretory lysosomes, as well as in a second population of lysosomes, which lack cathepsin K.

Gnptab$^{-/-}$ osteoclasts displayed similar cathepsin D-positive, electron-dense lysosomes (Figure 6C) as observed in WT cells (Figure 6A). In addition, cathepsin D was seen in the relatively electron-lucent organelles with trace amounts of cathepsin K representing endosomes and secretory lysosomes that failed to acquire their full content of cathepsin K in these cells (Figure 6C, for comparison see Figure 1G and I). In the TGN (Figure 6D, Figure S3) cathepsin D localized to small-sized vesicles that were more electron-lucent than the electron-dense cathepsin K-vesicles that are so abundant in these cells (Figure 1H, Figure 3A–B). Quantitative analysis of their TGN distributions confirmed that cathepsin D and K are packaged into different vesicles (Figure 6D), i.e. 63 ± 1.6% of biosynthetic cathepsin D vesicles did not contain cathepsin K. These data are consistent with the hypothesis that in the absence of Man-6-P modifications cathepsin K enters constitutive secretory vesicles while cathepsin D is sorted to lysosomes.

The intracellular distribution of cathepsin D and K was then analyzed by immunofluorescent staining in WT osteoclasts cultured on bone slices instead of plastic. In these bone resorbing osteoclasts, cathepsin D and K localized in distinct punctae (Figure 7), suggesting their predominant targeting to lysosomes and secretory lysosomes, respectively. Moreover, in these polarized cells, the cathepsin D punctae were found throughout the cytoplasm (Figure 7), while cathepsin K punctae concentrated within the actin ring (Figure 7, upper panel). These findings are consistent with the data obtained on non-resorbing osteoclasts, suggesting that cathepsin K is targeted to the ruffled border via secretory lysosomes.

DISCUSSION

It has been a matter of debate whether lysosomal hydrolases in osteoclasts are directly transported from the TGN to the ruffled border or first packaged into endo-lysosomes to be secreted in a regulated manner. A number of studies have presented data consistent with the acid hydrolases being targeted to the resorption lacuna via fusion of endo-lysosomal compartments with the ruffled border. Thus acid hydrolases, including cathepsin K and TRAP, have been detected by immunohistochemistry in intracellular vesicles, vacuoles and granules of osteoclasts, reminiscent of a lysosomal localization (13, 16, 27, 28), while biochemical studies showed that the processing of cathepsin K to its active form, which requires an acidic environment, occurs intracellularly (29, 30). Toyomura et al. found that in osteoclast precursor cells, LAMP-2 and the a3 isoform of V-ATPase were present in late endosomes and lysosomes, but upon differentiation into osteoclasts relocated to the plasma membrane, suggesting that these proteins are delivered to the ruffled border by fusion of lysosomes with the plasma membrane (15). In addition, Rab7, which is involved in the fusion of late endosomes and lysosomes, was found to localize to the ruffled border, together with the calcium sensor protein synaptotagmin VII, which regulates exocytosis of lysosomes (31, 32). Interestingly, depletion of either of these proteins impaired the secretion of cathepsin K and the bone resorptive function of the osteoclasts (31, 32). Together, these data suggest that secretion of active cathepsin K into the resorption lacuna may occur via fusion of secretory lysosomes, by a process mediated by Rab7 and synaptotagmin VII. However, the evidence for this pathway has remained indirect, since the actual presence of secretory lysosomes in osteoclasts and their fusion with the plasma membrane to discharge active cathepsin K and TRAP has not been clearly demonstrated. On the other hand, several

reports have suggested that secretion of the acid hydrolases into the resorption lacuna occurs via secretory vesicles derived directly from the TGN (9–11).

Our immuno-EM analysis of the subcellular distributions of cathepsin K and TRAP in osteoclasts provides, to our knowledge, the first evidence that these proteins co-localize in secretory lysosomes that release their content by fusion with the plasma membrane. Our biochemical studies showed that osteoclasts secrete processed, mature forms of cathepsin K and TRAP, which requires passage through the acidic environment of the lysosome. Moreover, we observed that the majority of the secreted acid hydrolases no longer contain the Man-6-P modification. These observations are consistent with the model that osteoclasts secrete mature lysosomal hydrolases via secretory lysosomes. Our data differ from those of Czupalla et al., who identified secretion of the proform of cathepsin D and of Man-6-P-containing lysosomal hydrolases as a major pathway (11). A possible explanation for this discrepancy is the dissimilar source for osteoclast differentiation, i.e. the myeloid cell line Raw 264.7 versus the bone-marrow derived macrophages that we used.

In addition to the issue of the pathway used to transport the lysosomal hydrolases to the ruffled border, the requirement of the Man-6-P targeting pathway in osteoclasts had never been addressed. Since disruption of the Man-6-P targeting pathway has different effects in tissues, e.g. fibroblasts and exocrine secretory tissues are highly affected (17, 18, 33), whereas other tissues (liver, muscle, brain) are spared, we evaluated the consequences in osteoclasts from *Gnptab*$^{-/-}$ mice, which are unable to synthesize the Man-6-P recognition moiety. Using osteoclasts from *Gnptab*$^{-/-}$ mice, we demonstrated that targeting of cathepsin K and TRAP to secretory lysosomes is Man-6-P-dependent. Based on these findings, we propose the following model (Figure 8). In osteoclasts, cathepsin K and TRAP receive Man-6-P modifications, which are required for MPR-binding at the TGN and subsequent trafficking to secretory lysosomes. Within the acidic environment of the secretory lysosomes, cathepsin K and TRAP are processed to their active forms, and subsequently released at the site of bone resorption by fusion of the secretory lysosomes with the ruffled border. In addition, substantial amounts of TRAP are secreted directly from the TGN. Cathepsin D also acquires Man-6-P modifications in osteoclasts but relatively low levels of this protease reach the cathepsin K- and TRAP-containing secretory lysosomes. The majority of cathepsin D is transported to a second class of lysosome that lacks cathepsin K and TRAP. Cathepsin D in secretory lysosomes may derive directly from the TGN and/or from fusion of secretory lysosomes with cathepsin D-enriched lysosomes. In *Gnptab*$^{-/-}$ osteoclasts (Figure 8, lower panel), the lack of the Man-6-P modification results in the secretion of the proforms of cathepsin K and TRAP directly from the TGN via the constitutive secretory pathway. Cathepsin D however, continues to reach lysosomes and secretory lysosomes, indicating that its transport is independent of the Man-6-P targeting system. Secretory lysosomes with reduced amounts of lysosomal hydrolases may still fuse with the ruffled border, resulting in acidification of the resorption lacuna and activation of the secreted proenzymes.

Our immuno-EM and biochemical studies were carried out on non-resorbing, non-polarized osteoclasts grown on a plastic substrate. Therefore we have not been able to address the trafficking of acid hydrolases at the different stages of bone resorption. It is possible that in addition to the fusion of secretory lysosomes with the ruffled border, the reuptake of acid hydrolases from the resorption lacuna could serve several roles. Thus the endocytosed hydrolases could assist in the degradation of endocytosed bone matrix fragments in transcytotic vesicles (7, 34, 35). In this regard, it is possible that acid hydrolases are directly targeted from the TGN to the transcytotic vesicles, as was suggested for TRAP (7, 34, 35). The endocytosed hydrolases could also be rerouted to secretory lysosomes to serve as a reservoir for when the osteoclasts move to the next location on the bone. It is important to

point out that osteoclasts cultured on a plastic substrate are considered a representative model of mature osteoclasts, despite their lack of polarization (36). Moreover, our immunofluorescence data obtained on osteoclasts grown on bone slices are consistent with our immuno-EM and biochemical data, showing that polarized osteoclasts have two populations of lysosomes, of which the cathepsin K-containing secretory lysosomes are targeted to the ruffled border.

The observation that cathepsin D is predominantly found in a second population of lysosomes negative for cathepsin K and TRAP is in accordance with previous immunohistochemical studies on bone resorbing osteoclasts showing that cathepsin D is barely detected at the ruffled border and that osteoclasts contain cathepsin D-positive and negative vacuoles (12, 26, 28). It remains to be established how the two subpopulations of lysosomes relate to each other regarding biogenesis and function.

Secretory lysosomes belong to the group of so-called lysosome-related organelles and occur mostly in cells derived from the hematopoietic lineage. Secretory lysosomes are thought to act as specialized lysosomes that store and release secretory proteins, while at the same time carrying out general lysosomal functions, thus acting as dual-functional organelles (21, 37). In the case of osteoclasts, it seems likely that the secretory lysosomes deliver acid hydrolases to the resorption lacuna, whereas the co-existing cathepsin D lysosomes ensure general lysosomal functions. However, we cannot rule out the possibility that the cathepsin D lysosomes fuse with the plasma membrane or with the secretory lysosomes. Also, they might represent residual lysosomes from the bone-marrow derived macrophages. Clearly, further studies are required to resolve this issue, as well as to elucidate the alternative mechanisms by which cathepsin D is targeted to these lysosomes in the absence of a functional Man-6-P sorting pathway. Man-6-P-independent lysosomal targeting of cathepsin D has previously been reported in several other cell types (38–41). Sortilin was recently proposed as an alternative receptor for cathepsin D and H (42, 43), but we could not detect this protein in osteoclast lysates by western blotting (data not shown). This raises the interesting possibility that in osteoclasts yet another lysosomal targeting pathway might exist.

In summary, our data show that osteoclasts contain a pathway for the regulated secretion of lysosomal hydrolases that involves targeting them to secretory lysosomes in a Man-6-P dependent manner followed by fusion of the secretory lysosomes with the plasma membrane. In addition, osteoclasts contain a second type of lysosomes enriched in the ubiquitously expressed lysosomal hydrolase cathepsin D. Disruption of the Man-6-P targeting parthway in *Gnptab*$^{-/-}$ osteoclasts leads to unregulated secretion of bone resorbing hydrolases, while cathepsin D continues to reach lysosomes in a Man-6-P-independent manner. It will be interesting to investigate in future studies whether the osteoporosis phenotype in *Gnptab*$^{-/-}$ mice (44), as well as in patients with mucolipidosis II (i.e. with mutations in *Gnptab*) (45–48), is the result, at least partially, of this abnormal secretion of acid hydrolases by osteoclasts.

MATERIALS AND METHODS

Antibodies and reagents

Chemicals were purchased from Sigma-Aldrich (St. Louis, MO) unless otherwise specified. The following antibodies were used: Mouse monoclonal antibodies against cathepsin K (Millipore, Billerica, MA) and GAPDH (Sigma-Aldrich, St. Louis, MO), rat monoclonal ABL-93 against LAMP-2 (Developmental Studies Hybridoma Bank, University of Iowa, Iowa City, IA), rabbit antibodies against cathepsin D (described in (49), CI-MPR (produced in S Kornfeld's laboratory), TRAP (generous gift from Dr RM Roberts, University of

Missouri, Columbia, MO), biotin (Rockland Immunochemicals, Inc., Gilbertsville, PA) and mouse immunoglobulins (DAKO, Heverlee, Belgium). The specificity of the cathepsin K and TRAP antibodies in immuno-EM was tested by immunogold labeling of WT bone-marrow macrophages, which do not express detectable levels of these proteins (50, 51) and accordingly did not show any label for cathepsin K or TRAP (Figure S4A–B). Man-6-P modified lysosomal acid hydrolases were detected with biotinylated, ligand binding domain of CI-MPR (sCI-MPR) (52), which was a generous gift from Dr P Lobel (Rutgers University, Piscataway, NJ). Lyophilized sCI-MPR was reconstituted to a final concentration of 10 μg/ml in PBS + 1% wt/vol BSA, containing 5 mM β-glycerol phosphate disodium salt pentahydrate and 0.02% wt/vol sodium azide (Merck, Darmstadt, Germany).

Cell culture

Bone-marrow derived macrophages were obtained from *Gnptab*$^{-/-}$ (17) and WT mice as described previously (31, 53). All animal procedures were carried out according to guidelines approved by the Animal Studies Committee of Washington University in St. Louis. Macrophages were cultured in α-MEM culture medium containing 10% FCS, 100 μg/ml penicillin and 100 units/ml streptomycin at 37°C in a 5% CO_2 humidified incubator, in the presence of 1/10 vol of CMG 14–12 culture supernatant-containing macrophage colony-stimulating factor (53). Osteoclast differentiation was induced by addition of 100 ng/ml GST linked receptor for activation of NF-κB ligand (RANK-L) for 4 to 6 days, until the cells reached confluency.

Immuno-EM

WT and *Gnptab*$^{-/-}$ osteoclasts were fixed with either 4% wt/vol PFA in 0.1 M phosphate buffer (PB) pH=7.4 or 0.2% wt/vol glutaraldehyde + 2% wt/vol PFA in 0.1 M PB (54). WT and *Gnptab*$^{-/-}$ macrophages were fixed with 4% wt/vol PFA in 0.1 M PB. Preparation of the samples, cryosectioning and immunogold labeling was performed as described (54). To label the endo-lysosomal system, cells were incubated with BSA conjugated to 5 nm gold particles (BSA-gold, Cell Microscopy Center, UMC Utrecht, the Netherlands) in α-MEM culture medium containing 1% FCS for 30 min or 3 h prior to fixation (55). Sections were analyzed in a JEOL 1200 EX electron microscope (Tokyo, Japan) at 80 kV.

Quantification of the number of secretory lysosomes and endosomes was performed in ultrathin cryosections of WT and *Gnptab*$^{-/-}$ osteoclasts labeled for cathepsin K (20 cell profiles each). Secretory lysosomes were defined as 200–900 nm cathepsin K-positive, electron-dense compartments. Endosomes as electron-lucent compartments with low levels of cathepsin K and few intraluminal vesicles. In *Gnptab*$^{-/-}$ osteoclasts all endosomes with low cathepsin K levels were counted as one category. The percentage of cathepsin K-positive vesicles containing BSA-gold after a 3 h incubation was determined by randomly screening sections of WT osteoclasts for cathepsin K-positive vesicles (defined as <200 nm) and scoring them as positive or negative for BSA-gold. 4 × 200 vesicles were counted, ± values are standard error of the mean. The percentage of co-localization between cathepsin K and cathepsin D was determined by counting 3 × 60 cathepsin D-positive, BSA-gold negative vesicles and scoring them positive or negative for cathepsin K, ± values are standard error of the mean.

Immunoblot analysis

Osteoclast media were collected after a 6 h incubation in the absence of serum. Cells were lysed in 1% Triton-X100/PBS, containing protease inhibitors (Roche Applied Science, Penzberg, Germany). Cell lysates and media samples were then resolved by SDS-PAGE and transferred onto a PVDF membrane for immunoblotting.

Lysosomal hydrolase sorting assay

WT and *Gnptab*$^{-/-}$ osteoclasts were subjected to pulse/chase labeling with TRAN ^{35}S-LABEL methionine/cysteine (MP Biomedicals LLC, Irvine, CA), as described (56). The percentage of secretion ± SD of TRAP (n=3) and cathepsin D (n=6) was determined after either a 30 min or 1.5 h pulse, followed by a 2 h chase. Similar experiments with cathepsin K were not performed due to the lack of an immunoprecipitating antibody.

Immunofluorescence

Cells were grown on glass coverslips or on bovine bone slices until they reached confluency, fixed in 4% wt/vol PFA in 0.1 M PB (pH=7.4) for 30 min at RT and permeabilized with 0.1% saponin in 2% BSA/PBS for 10 min. The primary antibodies were detected by Alexa FluorR 488-coupled anti-rabbit and Alexa FluorR 568-coupled anti-mouse or Cy5-coupled anti-mouse antibodies (Invitrogen, Molecular Probes, Carlsbad, CA), respectively. Actin was detected by with Alexa FluorR 488-phalloidin or TRITC-phalloidin and the coverslips were mounted with ProLong Gold antifade reagent (all from Invitrogen, Molecular Probes Carlsbad, CA). Analysis was performed under a Zeiss LSM 510 Meta confocal microscope (Sliedrecht, the Netherlands) using a 63x objective and equipped with a 32 PMT meta-detector or under a Deltavision RT fluorescence microscope with an Olympus 100x 1.4 numerical aperture objective and Cascade EMCCD camera. Z-stacks were deconvolved and processed using SoftWoRx software (Applied Precision, Issaquah, WA).

Lysosomal enzyme assays

Cells were lysed in 1% Triton-X100/PBS containing a protease inhibitor cocktail (Roche Applied Science, Penzberg, Germany). Samples were assayed for acid hydrolase activities using 4-methylumbellyferyl conjugated lysosomal hydrolase specific substrates as described (17, 56). Activities were expressed in nmol of hydrolyzed substrate/mg protein/h.

CI-MPR affinity chromatography

Osteoclasts were incubated for 6 h in serum free medium. The media were collected and the cells placed in column buffer (50 mM imidazole, pH=6.5, 150 mM NaCl, 1% Triton-X100) containing a protease inhibitor cocktail (Roche Applied Science, Penzberg, Germany) and disrupted by sonication. After centrifugation at 4°C for 10 min at 12 000 g, the cell lysates were diluted 1:2.5 in column buffer (containing 0.05% Triton-X100) and loaded onto the CI-MPR affinity column (0.5 mg CI-MPR per ml of Affigel-10), which was prepared as described previously (57). The media samples were directly applied onto the column. The flow through was collected and the column was washed first with 5 ml of column buffer and subsequently with 5 ml of column buffer containing 5 mM Glc-6-P to remove non-specifically bound hydrolases. Man-6-P-containing lysosomal hydrolases were eluted from the column by addition of 5 ml of column buffer containing 10 mM Man-6-P. Fractions of one ml were collected and assayed for lysosomal hydrolase activities as described. The amount of acid hydrolases that specifically bound to the column (Man-6-P eluted fraction) was then expressed as a percentage of the total recovered activity.

Supplementary Material

Refer to Web version on PubMed Central for supplementary material.

Acknowledgments

We thank all our colleagues for helpful discussions and suggestions. We thank Carl DeSelm and Jean Chappel for their help with culturing the osteoclasts, René Scriwanek and Marc van Peski for preparation of the electron micrographs and drawings, Guojun Bu and Takahisa Kanekiyo for their help with the confocal microscopy and

Hans Geuze for critically reading the manuscript. EvM and JK were supported by VICI grant 918.56.611 of the Netherlands Organization for Scientific Research (NWO). MB and SK were supported by NIH grant CA 008759-44. HZ was supported by NIH grant AR 055694, and HZ and PR by grants AR 032788 and AR 046523 to Dr. Steven L. Teitelbaum. This work was further supported by an internationalization grant of the University Medical Center Utrecht, the Netherlands, to EvM and JK. The funders had no role in study design, data collection and analysis, decision to publish, or preparation of the manuscript.

ABBREVIATIONS LIST

CI-MPR	cation-independent mannose 6-phosphate receptor
Gnptab	gene encoding GlcNAc-1-phosphotransferase α,β-subunits
Man-6-P	mannose 6-phosphate
nm	nanometer
PB	phosphate buffer
TRAP	tartrate-resistant acid phosphatase
WT	wild type

References

1. Coxon FP, Taylor A. Vesicular trafficking in osteoclasts. Semin Cell Dev Biol. 2008; 19(5):424–433. [PubMed: 18768162]
2. Teitelbaum SL. Bone resorption by osteoclasts. Science. 2000; 289(5484):1504–1508. [PubMed: 10968780]
3. Vaananen HK, Zhao H, Mulari M, Halleen JM. The cell biology of osteoclast function. J Cell Sci. 2000; 113 (Pt 3):377–381. [PubMed: 10639325]
4. Bossard MJ, Tomaszek TA, Thompson SK, Amegadzie BY, Hanning CR, Jones C, Kurdyla JT, McNulty DE, Drake FH, Gowen M, Levy MA. Proteolytic activity of human osteoclast cathepsin K. Expression, purification, activation, and substrate identification. J Biol Chem. 1996; 271(21): 12517–12524. [PubMed: 8647860]
5. Bromme D, Okamoto K, Wang BB, Biroc S. Human cathepsin O2, a matrix protein-degrading cysteine protease expressed in osteoclasts. Functional expression of human cathepsin O2 in Spodoptera frugiperda and characterization of the enzyme. J Biol Chem. 1996; 271(4):2126–2132. [PubMed: 8567669]
6. Angel NZ, Walsh N, Forwood MR, Ostrowski MC, Cassady AI, Hume DA. Transgenic mice overexpressing tartrate-resistant acid phosphatase exhibit an increased rate of bone turnover. J Bone Miner Res. 2000; 15(1):103–110. [PubMed: 10646119]
7. Halleen JM, Raisanen S, Salo JJ, Reddy SV, Roodman GD, Hentunen TA, Lehenkari PP, Kaija H, Vihko P, Vaananen HK. Intracellular fragmentation of bone resorption products by reactive oxygen species generated by osteoclastic tartrate-resistant acid phosphatase. J Biol Chem. 1999; 274(33): 22907–22910. [PubMed: 10438453]
8. Sun P, Sleat DE, Lecocq M, Hayman AR, Jadot M, Lobel P. Acid phosphatase 5 is responsible for removing the mannose 6-phosphate recognition marker from lysosomal proteins. Proc Natl Acad Sci U S A. 2008; 105(43):16590–16595. [PubMed: 18940929]
9. Baron R, Neff L, Brown W, Courtoy PJ, Louvard D, Farquhar MG. Polarized secretion of lysosomal enzymes: co-distribution of cation-independent mannose-6-phosphate receptors and lysosomal enzymes along the osteoclast exocytic pathway. J Cell Biol. 1988; 106(6):1863–1872. [PubMed: 2968345]
10. Baron R, Neff L, Louvard D, Courtoy PJ. Cell-mediated extracellular acidification and bone resorption: evidence for a low pH in resorbing lacunae and localization of a 100-kD lysosomal membrane protein at the osteoclast ruffled border. J Cell Biol. 1985; 101(6):2210–2222. [PubMed: 3905822]

11. Czupalla C, Mansukoski H, Riedl T, Thiel D, Krause E, Hoflack B. Proteomic analysis of lysosomal acid hydrolases secreted by osteoclasts: implications for lytic enzyme transport and bone metabolism. Mol Cell Proteomics. 2006; 5(1):134–143. [PubMed: 16215273]
12. Goto T, Yamaza T, Tanaka T. Cathepsins in the osteoclast. J Electron Microsc (Tokyo). 2003; 52(6):551–558. [PubMed: 14756243]
13. Littlewood-Evans A, Kokubo T, Ishibashi O, Inaoka T, Wlodarski B, Gallagher JA, Bilbe G. Localization of cathepsin K in human osteoclasts by in situ hybridization and immunohistochemistry. Bone. 1997; 20(2):81–86. [PubMed: 9028530]
14. Mulari M, Vaaraniemi J, Vaananen HK. Intracellular membrane trafficking in bone resorbing osteoclasts. Microsc Res Tech. 2003; 61(6):496–503. [PubMed: 12879417]
15. Toyomura T, Murata Y, Yamamoto A, Oka T, Sun-Wada GH, Wada Y, Futai M. From lysosomes to the plasma membrane: localization of vacuolar-type H+-ATPase with the a3 isoform during osteoclast differentiation. J Biol Chem. 2003; 278(24):22023–22030. [PubMed: 12672822]
16. Yamaza T, Goto T, Kamiya T, Kobayashi Y, Sakai H, Tanaka T. Study of immunoelectron microscopic localization of cathepsin K in osteoclasts and other bone cells in the mouse femur. Bone. 1998; 23(6):499–509. [PubMed: 9855458]
17. Gelfman CM, Vogel P, Issa TM, Turner CA, Lee WS, Kornfeld S, Rice DS. Mice lacking alpha/beta subunits of GlcNAc-1-phosphotransferase exhibit growth retardation, retinal degeneration, and secretory cell lesions. Invest Ophthalmol Vis Sci. 2007; 48(11):5221–5228. [PubMed: 17962477]
18. Lee WS, Payne BJ, Gelfman CM, Vogel P, Kornfeld S. Murine UDP-GlcNAc:lysosomal enzyme N-acetylglucosamine-1-phosphotransferase lacking the gamma-subunit retains substantial activity toward acid hydrolases. J Biol Chem. 2007; 282(37):27198–27203. [PubMed: 17652091]
19. Holt OJ, Gallo F, Griffiths GM. Regulating secretory lysosomes. J Biochem. 2006; 140(1):7–12. [PubMed: 16877763]
20. Sachse M, Ramm G, Strous G, Klumperman J. Endosomes: multipurpose designs for integrating housekeeping and specialized tasks. Histochem Cell Biol. 2002; 117(2):91–104. [PubMed: 11935285]
21. Blott EJ, Griffiths GM. Secretory lysosomes. Nat Rev Mol Cell Biol. 2002; 3(2):122–131. [PubMed: 11836514]
22. Peters PJ, Borst J, Oorschot V, Fukuda M, Krahenbuhl O, Tschopp J, Slot JW, Geuze HJ. Cytotoxic T lymphocyte granules are secretory lysosomes, containing both perforin and granzymes. J Exp Med. 1991; 173(5):1099–1109. [PubMed: 2022921]
23. Klumperman J, Hille A, Veenendaal T, Oorschot V, Stoorvogel W, von Figura K, Geuze HJ. Differences in the endosomal distributions of the two mannose 6-phosphate receptors. J Cell Biol. 1993; 121(5):997–1010. [PubMed: 8099077]
24. van Meel E, Klumperman J. Imaging and imagination: understanding the endo-lysosomal system. Histochem Cell Biol. 2008; 129(3):253–266. [PubMed: 18274773]
25. Ljusberg J, Wang Y, Lang P, Norgard M, Dodds R, Hultenby K, Ek-Rylander B, Andersson G. Proteolytic excision of a repressive loop domain in tartrate-resistant acid phosphatase by cathepsin K in osteoclasts. J Biol Chem. 2005; 280(31):28370–28381. [PubMed: 15929988]
26. Goto T, Tsukuba T, Ayasaka N, Yamamoto K, Tanaka T. Immunocytochemical localization of cathepsin D in the rat osteoclast. Histochemistry. 1992; 97(1):13–18. [PubMed: 1618634]
27. Reinholt FP, Hultenby K, Heinegard D, Marks SC Jr, Norgard M, Anderson G. Extensive clear zone and defective ruffled border formation in osteoclasts of osteopetrotic (ia/ia) rats: implications for secretory function. Exp Cell Res. 1999; 251(2):477–491. [PubMed: 10471332]
28. Goto T, Kiyoshima T, Moroi R, Tsukuba T, Nishimura Y, Himeno M, Yamamoto K, Tanaka T. Localization of cathepsins B, D, and L in the rat osteoclast by immuno-light and -electron microscopy. Histochemistry. 1994; 101(1):33–40. [PubMed: 8026981]
29. Dodds RA, James IE, Rieman D, Ahern R, Hwang SM, Connor JR, Thompson SD, Veber DF, Drake FH, Holmes S, Lark MW, Gowen M. Human osteoclast cathepsin K is processed intracellularly prior to attachment and bone resorption. J Bone Miner Res. 2001; 16(3):478–486. [PubMed: 11277265]

30. Rieman DJ, McClung HA, Dodds RA, Hwang SM, Holmes MW, James IE, Drake FH, Gowen M. Biosynthesis and processing of cathepsin K in cultured human osteoclasts. Bone. 2001; 28(3):282–289. [PubMed: 11248658]
31. Zhao H, Ito Y, Chappel J, Andrews NW, Teitelbaum SL, Ross FP. Synaptotagmin VII regulates bone remodeling by modulating osteoclast and osteoblast secretion. Dev Cell. 2008; 14(6):914–925. [PubMed: 18539119]
32. Zhao H, Laitala-Leinonen T, Parikka V, Vaananen HK. Downregulation of small GTPase Rab7 impairs osteoclast polarization and bone resorption. J Biol Chem. 2001; 276(42):39295–39302. [PubMed: 11514537]
33. Boonen M, van Meel E, Oorschot V, Klumperman J, Kornfeld S. Vacuolization of mucolipidosis type II mouse exocrine gland cells represents accumulation of autolysosomes. Mol Biol Cell. 2011
34. Nesbitt SA, Horton MA. Trafficking of matrix collagens through bone-resorbing osteoclasts. Science. 1997; 276(5310):266–269. [PubMed: 9092478]
35. Salo J, Lehenkari P, Mulari M, Metsikko K, Vaananen HK. Removal of osteoclast bone resorption products by transcytosis. Science. 1997; 276(5310):270–273. [PubMed: 9092479]
36. Lacey DL, Timms E, Tan HL, Kelley MJ, Dunstan CR, Burgess T, Elliott R, Colombero A, Elliott G, Scully S, Hsu H, Sullivan J, Hawkins N, Davy E, Capparelli C, et al. Osteoprotegerin ligand is a cytokine that regulates osteoclast differentiation and activation. Cell. 1998; 93(2):165–176. [PubMed: 9568710]
37. Griffiths GM, Isaaz S. Granzymes A and B are targeted to the lytic granules of lymphocytes by the mannose-6-phosphate receptor. J Cell Biol. 1993; 120(4):885–896. [PubMed: 8432729]
38. Dittmer F, Ulbrich EJ, Hafner A, Schmahl W, Meister T, Pohlmann R, von Figura K. Alternative mechanisms for trafficking of lysosomal enzymes in mannose 6-phosphate receptor-deficient mice are cell type-specific. J Cell Sci. 1999; 112 (Pt 10):1591–1597. [PubMed: 10212152]
39. Glickman JN, Kornfeld S. Mannose 6-phosphate-independent targeting of lysosomal enzymes in I-cell disease B lymphoblasts. J Cell Biol. 1993; 123(1):99–108. [PubMed: 8408210]
40. Rijnboutt S, Aerts HM, Geuze HJ, Tager JM, Strous GJ. Mannose 6-phosphate-independent membrane association of cathepsin D, glucocerebrosidase, and sphingolipid-activating protein in HepG2 cells. J Biol Chem. 1991; 266(8):4862–4868. [PubMed: 1848227]
41. Rijnboutt S, Kal AJ, Geuze HJ, Aerts H, Strous GJ. Mannose 6-phosphate-independent targeting of cathepsin D to lysosomes in HepG2 cells. J Biol Chem. 1991; 266(35):23586–23592. [PubMed: 1660878]
42. Canuel M, Korkidakis A, Konnyu K, Morales CR. Sortilin mediates the lysosomal targeting of cathepsins D and H. Biochem Biophys Res Commun. 2008; 373(2):292–297. [PubMed: 18559255]
43. Lefrancois S, Canuel M, Zeng J, Morales CR. Inactivation of sortilin (a novel lysosomal sorting receptor) by dominant negative competition and RNA interference. Biol Proced Online. 2005; 7:17–25. [PubMed: 15682222]
44. Vogel P, Payne BJ, Read R, Lee WS, Gelfman CM, Kornfeld S. Comparative pathology of murine mucolipidosis types II and IIIC. Vet Pathol. 2009; 46(2):313–324. [PubMed: 19261645]
45. Hochman JA, Treem WR, Dougherty F, Bentley RC. Mucolipidosis II (I-cell disease) presenting as neonatal cholestasis. J Inherit Metab Dis. 2001; 24(5):603–604. [PubMed: 11757590]
46. Kabra M, Gulati S, Kaur M, Sharma J, Singh A, Chopra V, Menon PS, Kalra V. I-cell disease (Mucolipidosis II). Indian J Pediatr. 2000; 67(9):683–687. [PubMed: 11028124]
47. Patriquin HB, Kaplan P, Kind HP, Giedion A. Neonatal mucolipidosis II (I-cell disease): clinical and radiologic features in three cases. AJR Am J Roentgenol. 1977; 129(1):37–43. [PubMed: 409140]
48. Pazzaglia UE, Beluffi G, Campbell JB, Bianchi E, Colavita N, Diard F, Gugliantini P, Hirche U, Kozlowski K, Marchi A, et al. Mucolipidosis II: correlation between radiological features and histopathology of the bones. Pediatr Radiol. 1989; 19(6–7):406–413. [PubMed: 2771479]
49. Glickman JN, Morton PA, Slot JW, Kornfeld S, Geuze HJ. The biogenesis of the MHC class II compartment in human I-cell disease B lymphoblasts. J Cell Biol. 1996; 132(5):769–785. [PubMed: 8603911]

50. Filgueira L. Fluorescence-based staining for tartrate-resistant acidic phosphatase (TRAP) in osteoclasts combined with other fluorescent dyes and protocols. J Histochem Cytochem. 2004; 52(3):411–414. [PubMed: 14966208]
51. Kamiya T, Kobayashi Y, Kanaoka K, Nakashima T, Kato Y, Mizuno A, Sakai H. Fluorescence microscopic demonstration of cathepsin K activity as the major lysosomal cysteine proteinase in osteoclasts. J Biochem. 1998; 123(4):752–759. [PubMed: 9538271]
52. Valenzano KJ, Kallay LM, Lobel P. An assay to detect glycoproteins that contain mannose 6-phosphate. Anal Biochem. 1993; 209(1):156–162. [PubMed: 8465950]
53. Takeshita S, Kaji K, Kudo A. Identification and characterization of the new osteoclast progenitor with macrophage phenotypes being able to differentiate into mature osteoclasts. J Bone Miner Res. 2000; 15(8):1477–1488. [PubMed: 10934646]
54. Slot JW, Geuze HJ. Cryosectioning and immunolabeling. Nat Protoc. 2007; 2(10):2480–2491. [PubMed: 17947990]
55. de Wit H, Lichtenstein Y, Geuze HJ, Kelly RB, van der Sluijs P, Klumperman J. Synaptic vesicles form by budding from tubular extensions of sorting endosomes in PC12 cells. Mol Biol Cell. 1999; 10(12):4163–4176. [PubMed: 10588650]
56. Boonen M, Vogel P, Platt KA, Dahms N, Kornfeld S. Mice lacking mannose 6-phosphate uncovering enzyme activity have a milder phenotype than mice deficient for N-acetylglucosamine-1-phosphotransferase activity. Mol Biol Cell. 2009; 20(20):4381–4389. [PubMed: 19710420]
57. Varki A, Kornfeld S. The spectrum of anionic oligosaccharides released by endo-beta-N-acetylglucosaminidase H from glycoproteins. Structural studies and interactions with the phosphomannosyl receptor. J Biol Chem. 1983; 258(5):2808–2818. [PubMed: 6298207]

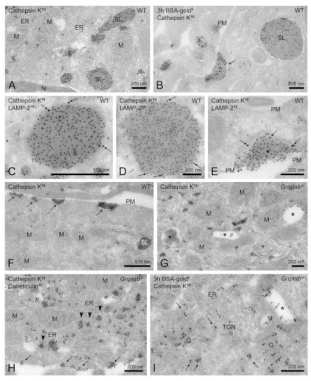

Figure 1. Ultrastructural localization of cathepsin K in WT and *Gnptab*$^{-/-}$ mouse osteoclasts

(A–F) Ultrathin cryosections of WT osteoclasts. Cathepsin K (10 nm gold particles) localizes to secretory lysosomes (A), which are reached by BSA-gold (5nm) after a 3 h uptake (B), contain LAMP-2 (15 nm, indicated by arrows) on their limiting membrane (C–D) and fuse with the plasma membrane (arrows in F). LAMP-2 is also present on the plasma membrane underlying the secreted patches of cathepsin K (E, asterisk). Arrow in B shows a BSA-gold/cathepsin K positive patch at the plasma membrane. (G–I) Ultrathin cryosections of *Gnptab*$^{-/-}$ osteoclasts. (G) Cathepsin K labeling (10 nm) in endo-lysosomal compartments (asterisks) was reduced, while more was found in small vesicles that typically lacked the ER marker calreticulin (15 nm) (H, arrowheads). Arrows point to small cathepsin K patches at the plasma membrane. (I) Most cathepsin K (10 nm) containing vesicles are inaccessible to BSA-gold (5 nm) after a 3 h uptake (arrows). Asterisk, endosomal compartment with low amounts of cathepsin K.

E, endosome; G, Golgi complex; M, mitochondrion; N, nucleus; PM, plasma membrane; SL, secretory lysosome.

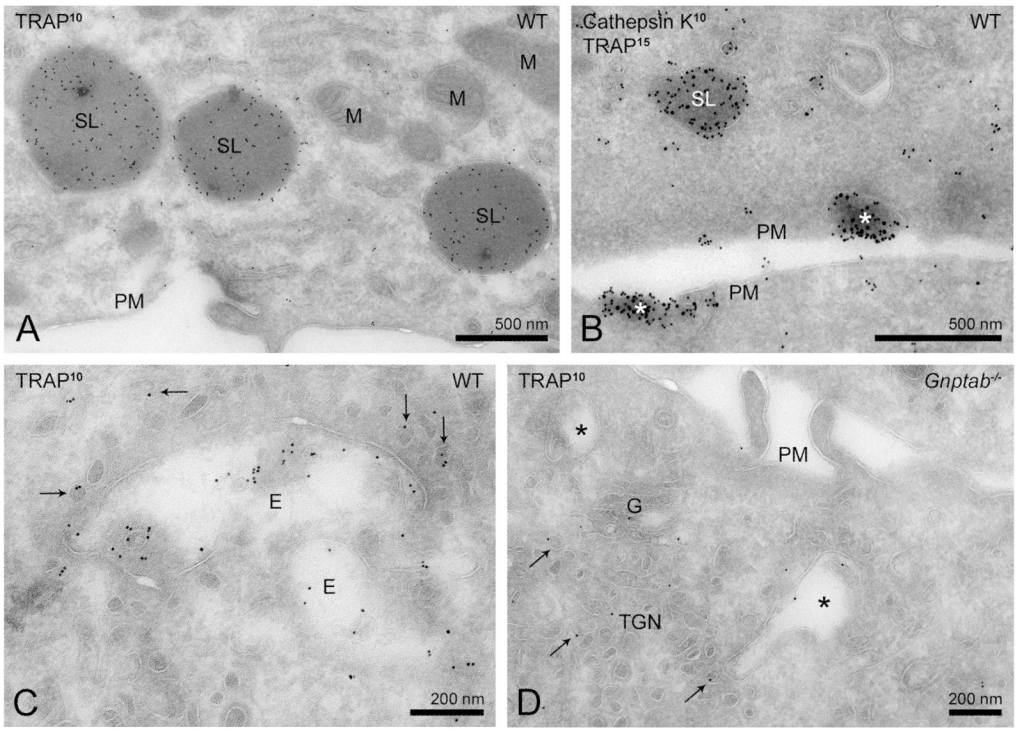

Figure 2. Ultrastructural localization of TRAP in WT and *Gnptab*$^{-/-}$ mouse osteoclasts

(A–C) Ultrathin cryosections of WT osteoclasts. TRAP localizes to secretory lysosomes (A) that also contain cathepsin K (B) and fuse with the plasma membrane (B, asterisks). (C) Low but consistent labeling of TRAP is present in endosomes and vesicles in close proximity (arrows). (D) TRAP labeling is virtually absent from endo-lysosomal compartments (asterisks) of *Gnptab*$^{-/-}$ osteoclasts, but low labeling of the Golgi and TGN is detected (arrows).

E, endosome; G, Golgi complex; M, mitochondrion; PM, plasma membrane; SL, secretory lysosome.

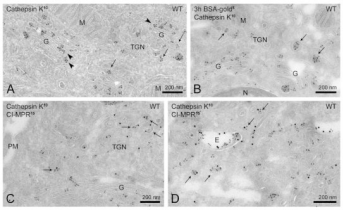

Figure 3. Cathepsin K co-localizes with CI-MPR in the TGN and early endosomes of mouse WT osteoclasts

(A–D) Ultrathin cryosections of WT osteoclasts. (A) Cathepsin K concentrates locally in Golgi cisternae (arrowheads) and TGN vesicles (arrows). (B) Cathepsin K-containing vesicles in the TGN area are mostly devoid of BSA-gold after 3 h of uptake (arrows). (C–D) Cathepsin K (10 nm) and CI-MPR (15 nm) co-localize in TGN vesicles (C, arrows), endosomes and vesicles in close proximity (D, arrows).

E, endosome; G, Golgi complex; M, mitochondrion; N, nucleus; PM, plasma membrane.

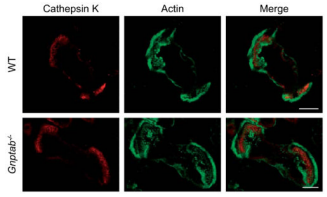

Figure 4. Cathepsin K is still targeted to the ruffled border in *Gnptab*$^{-/-}$ mice

The immunofluorescent staining for cathepsin K (red) and actin (green) on WT (upper panel) and *Gnptab*$^{-/-}$osteoclasts (lower panel) grown on bone slices shows that cathepsin K concentrates inside the actin rings formed by both cell types. Bars, 20 μm.

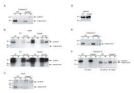

Figure 5. Targeting of cathepsin K and TRAP to secretory lysosomes is Man-6-P dependent, while cathepsin D sorting is Man-6-P-independent

(A, C–E) Steady state levels of cathepsin K (A), TRAP (C) and cathepsin D (E) shown by western blotting of cell lysates (lanes 1 and 3) and media (lanes 2 and 4) of WT and *Gnptab*$^{-/-}$ osteoclasts. * in (E) indicates a non-specific band. (D) GAPDH was detected in the cell lysates to confirm that equal protein amounts were loaded. Note that the GAPDH control applies for all three western blots, as equal amounts of each cell sample were loaded for each blot. (B) WT or *Gnptab*$^{-/-}$ osteoclasts were incubated for 30 min with ^{35}S-methionine/cysteine (pulse) and subsequently chased in unlabeled medium. TRAP was immunoprecipitated in cells and media collected directly after the pulse (30′) or at the end of the 2 h chase period (30′+2h). The upper panel and the lower panel show respectively a short (1day) and a long (7 days) exposure period of the same gel (reducing conditions). Note the appearance of a ~23 kD band, corresponding to mature TRAP (N-terminal fragment) in WT lysates and medium after the 2 h chase. * indicates a non-specific band. (F) Cathepsin D was immunoprecipitated either directly after the 30 min pulse or after a 4 h chase, resolved by SDS-PAGE under non-reducing conditions, and visualized by autoradiography. C, cell lysate, M, medium.

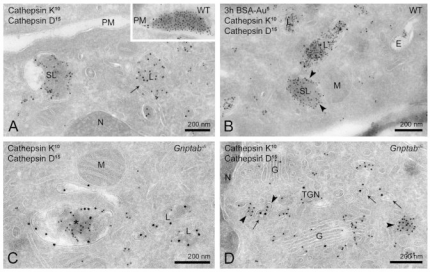

Figure 6. Cathepsin D localizes to a second type of lysosome that is cathepsin K-negative

Double immunogold labeling for cathepsin K (10 nm) and cathepsin D (15 nm) in WT (A–B) and *Gnptab*$^{-/-}$ (C–D) osteoclasts. (A) Low but consistent levels of cathepsin D are found in cathepsin K-positive secretory lysosomes that fuse with the plasma membrane (inset in A). In addition, cathepsin D is detected in lysosomes that are devoid of cathepsin K (A, arrow). (B) Both secretory lysosomes and cathepsin D lysosomes are reached by BSA-gold (5 nm) after 3 h of uptake. Arrowheads indicate BSA-gold in a cathepsin K-positive secretory lysosome. (C) In *Gnptab*$^{-/-}$ cells, cathepsin D localizes to lysosomes and secretory lysosomes with reduced amounts of cathepsin K (asterisk). (D) In the TGN of *Gnptab*$^{-/-}$ osteoclasts, cathepsin D (arrows) and cathepsin K (arrowheads) are sorted into distinct types of vesicles.

E, endosome; G, Golgi complex; L, lysosome; M, mitochondrion; N, nucleus; PM, plasma membrane; SL, secretory lysosome.

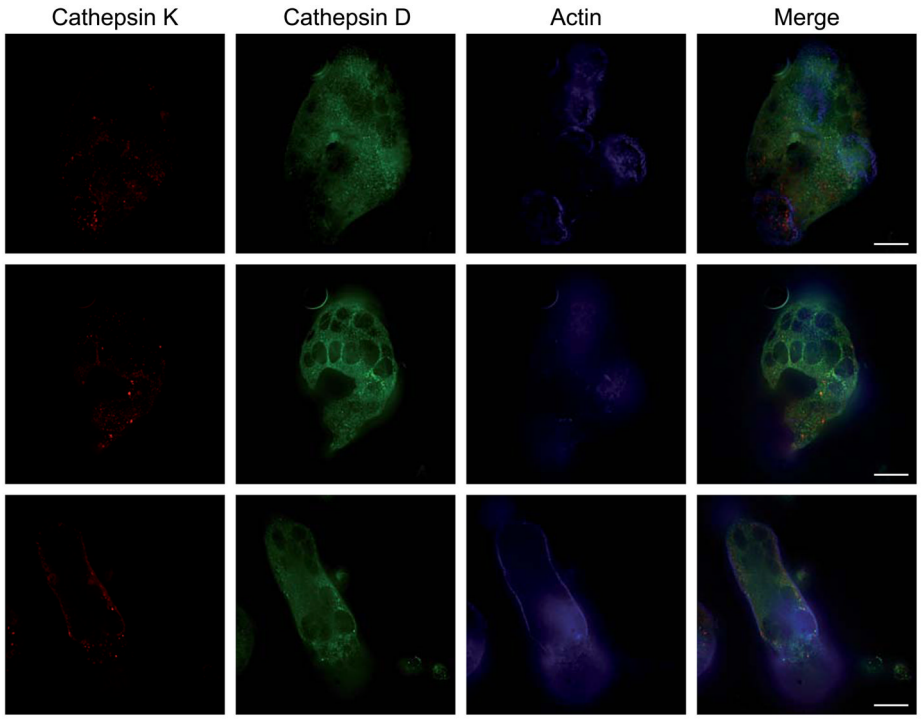

Figure 7. WT osteoclasts grown on bone show differential staining patterns for cathepsin K and D

WT osteoclasts grown on bone were fluorescently stained for cathepsin K (red), cathepsin D (green) and actin (blue). Cathepsin K-containing secretory lysosomes localize within the actin ring (upper panels). Cathepsin D-containing lysosomes are distributed throughout the cytoplasm (middle panels; same cell as upper panels but at a plane away from the ruffled border). Lower panels show a different cell, in which cathepsin K and D localize to distinct lysosomes. Bars, 10 μm.

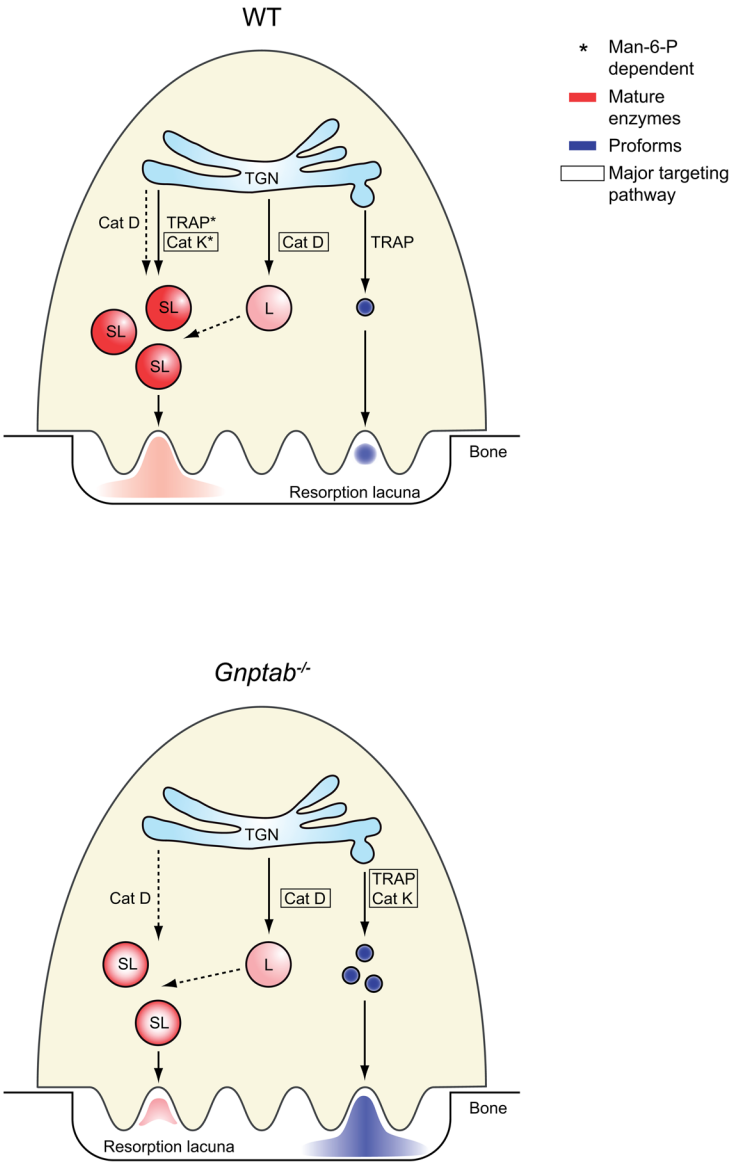

Figure 8. Trafficking of cathepsin K, TRAP and cathepsin D in mouse osteoclasts

See discussion for details. The asterisks indicate the transport mechanisms that are Man-6-P-dependent. The colors red and blue represent the active lysosomal hydrolases or their inactive proforms, respectively. When several transport routes are possible, the major pathway is indicated by a box.